Asian Journal of Chemistry; Vol. 37, No. 10 (2025), 2471-2476
ASIAN JOURNAL OF CHEMISTRY
https://doi.org/10.14233/ajchem.2025.34392

# Synthesis, Characterization and Agronomic Evaluation of ZnO Nanoparticles using Solution Combustion Method

KAILA SINDHUJA[1], CH. ASHOK[2], CH. SHILPA CHAKRA[1], T. BALA NARSAIAH[3], LAKSHMANA NAIK RAMAVATHU[4,*] and P. AKHILA SWATHANTHRA[5]

[1]Centre for Chemical Sciences and Technology, JNTUH University College of Engineering, Science & Technology, Hyderabad-500085, India
[2]Nanospan India Pvt Ltd, Hyderabad-502319, India
[3]Department of Chemical Engineering, JNTUA College of Engineering-Anantapur, Anantapuramu-515002, India
[4]Department of Chemical Engineering, Indian Institute of Technology Jodhpur, Jodhpur-342030, India
[5]Department of Chemical Engineering, Sri Venkateswara University College of Engineering, Tirupati-517502, India

*Corresponding author: E-mail: lakshman2027@gmail.com

*Received*: 3 July 2025 *Accepted*: 13 September 2025 *Published online*: 30 September 2025 AJC-22131

Metal oxides, particularly zinc oxide (ZnO), have sparked widespread interest due to their unique properties. The current research focuses on the solution combustion method for the synthesis of zinc oxide nanoparticles (ZnO NPs), with zinc nitrate as oxidizing agent and ascorbic acid as precursor. The resulting ZnO NPs were analyzed for their crystal structure, particle size, morphology, elemental composition and thermal behaviour using various characterization techniques, including X-ray diffraction (XRD), particle size analysis (PSA), scanning electron microscopy (SEM), energy-dispersive X-ray spectroscopy (EDS) and thermogravimetric-differential thermal analysis (TG/DTA). Furthermore, the synthesized ZnO NPs were applied to assess their impact on the germination and growth of *Vigna radiata* (mung bean) seeds. Exposure of *V. radiata* to varying concentrations of ZnO nanoparticles revealed a concentration-dependent enhancement in plant growth, with the highest height of 29.5 cm observed in Pot-4 by day 20. These results suggest that moderate ZnO NPs applications may stimulate plant development, offering potential agronomic benefits under controlled conditions.

**Keywords: ZnO NPs, Solution combustion method, Phototoxicity, Germination, *Vigna radiata*.**

## INTRODUCTION

Nanoparticles possess unique properties especially a high surface area-to-volume ratio and tunable surface chemistry that make them valuable across a wide range of applications [1,2]. Zinc oxide nanoparticles (ZnO NPs) have attracted significant research interest due to their multifunctional properties, including photocatalytic activity, UV-blocking ability, and antimicrobial effects [3,4]. As a result, ZnO NPs are used in an industry, including medicine, cosmetics, food packaging and most recently, in agriculture [5-7]. The integration of nanoparticles in agriculture, often termed "nano-agriculture" has opened new avenues for improving crop yield, disease management and nutrient delivery. The applications of ZnO NPs in agriculture holds promise for enhancing plant productivity and ability to withstand both biotic and abiotic stresses [8]. ZnO is regarded as a micronutrient that is necessary for several plant enzymatic and metabolic functions and due to their nanoscale size, ZnO NPs provide a more effective delivery method. According to reports, when applied in the right amounts, ZnO NPs can boost nutrient absorption, promote seed germination and improve plant development [9,10]. Furthermore, ZnO NPs have antifungal and antibacterial properties that can help in defending crops against infections [11]. This dual role of ZnO NPs as a micronutrient source and antimicrobial agent makes them attractive for sustainable agricultural practices.

However, the increased usage of nanoparticles, especially metal oxides like ZnO, has also raised concerns about their environmental fate and potential toxicity to living organisms, particularly plants [12]. Consequently, the phytotoxicity of ZnO NPs has gained increasing attention [12]. Phytotoxicity refers to harmful effects on plant growth and development, which ZnO NPs may cause through mechanisms such as generating

reactive oxygen species (ROS), hindering water and nutrient uptake and disrupting essential processes like photosynthesis and transpiration [13,14]. Understanding the interactions of ZnO NPs within plant systems is crucial for assessing their potential risks in agricultural applications [15]. However, the potential benefits of ZnO NPs are accompanied by the risk of toxicity if not applied within optimal concentrations. Excessive exposure can induce phytotoxic effects, adversely impacting the plant growth and yield [16]. The interaction between nanoparticles and plant tissues is complex and can depend on nanoparticle concentration, shape, size, charge on surface and the plant involved.

*Vigna radiata* (mung bean) is a widely cultivated legume in tropical and subtropical regions, valued for its high protein content and its role in improving soil fertility through atmospheric nitrogen fixation. Due to its nutritional and economic significance, it serves as a suitable model for evaluating the impact of environmental stressors, including nanoparticle exposure. Research on the phytotoxicity of ZnO NPs in *V. radiata* is particularly important, as legumes form symbiotic relationships with nitrogen-fixing bacteria in root nodules. Disruption of root function by ZnO NPs toxicity could impair this synergy, ultimately affecting plant growth and yield. Therefore, assessing the effects of ZnO NPs on *V. radiata* is essential for understanding their broader implications in agricultural systems.

The aim of this study is to evaluate the phytotoxic effects of ZnO NPs on the growth and development of *V. radiata*. Specifically, the research investigates the influence of varying ZnO NPs concentrations on seed germination, root and shoot elongation and overall plant health. By assessing these key parameters, the study seeks to provide insights into the potential risks associated with the agricultural use of ZnO NPs. Furthermore, the findings will contribute to a better understanding of nanoparticle interactions with leguminous crops, which are essential for sustainable agriculture due to their nitrogen-fixing ability and soil fertility enhancement. The synthesized ZnO NPs were characterized using XRD, PSA, SEM, EDS, TG-DTA and subsequently applied to assess their impact on *V. radiata* seed germination and early growth.

## EXPERIMENTAL

**Preparation of ZnO NPs:** Zinc nitrate (oxidizer) and ascorbic acid (fuel) were used as precursors for the synthesis of ZnO NPs. Dissolved 0.594 g of zinc nitrate in 100 mL of distilled water while stirring for 15 min followed by the addition of 0.176 g of ascorbic acid and stirred continuously for another 15 min. The mixture was then placed on a hot plate maintained at 300 ºC. During the reaction process, observable phenomena such as boiling, frothing, smoldering, flaming, and fuming occurred, ultimately leading to the formation of ZnO nanopowder. The resulting ZnO nanoparticles were collected and subjected to further characterization.

**Characterization:** Powder X-ray diffraction (XRD) patterns were obtained using a Rigaku Denki RINT 2500 diffractometer with Cu*K*α radiation. The morphology of the synthesized ZnO NPs was examined using scanning electron microscopy (SEM, Philips XL30), while their elemental composition was analyzed through energy-dispersive X-ray spectroscopy (EDS) using a MIRA3 instrument (TES-CAN, Czech Republic). Fourier Transform Infrared (FTIR) spectra were recorded using a JASCO FT/IR-660 Plus 15 spectrometer employing the KBr pellet method. TGA/DTA experiments were carried out using Setaram SETSYS-16/18 on finely ground powders in air atmosphere between 30 and 800 ºC with a heating rate of 5 ºC/min.

**Mung bean growth conditions:** To evaluate the effects of ZnO NPs on mung bean (*V. radiata*) seed growth, four beakers (Beaker-1 to Beaker-4) were prepared, each containing 20 mL of distilled water and 10 seeds [17,18]. ZnO NPs were added to Beakers 2, 3 and 4 at varying concentrations to assess different exposure levels, while Beaker-1 served as the control.

Beaker-1: 20 mL distilled water + 10 Mung bean seeds (control group).

Beaker-2: 20 mL distilled water + 10 Mung bean seeds + 0.01 g of ZnO.

Beaker-3: 20 mL distilled water + 10 Mung bean seeds + 0.02 g of ZnO.

Beaker-4: 20 mL distilled water + 10 Mung bean seeds + 0.03 g of ZnO.

The beakers were subjected to sonication for 30 min to disperse the ZnO NPs and facilitate seed treatment. Seeds were then soaked for 6 h to allow adequate nanoparticle exposure. Following the soaking period, the seeds were individually planted in separate pots labeled as follows: Pot-1: seeds soaked in Beaker-1; Pot-2: seeds soaked in Beaker-2; Pot-3: seeds soaked in Beaker-3; and Pot-4: seeds soaked in Beaker-4.

## RESULTS AND DISCUSSION

**XRD studies:** The XRD pattern shown in Fig. 1 confirms the successful synthesis of ZnO NPs. The observed diffraction peaks correspond to the standard JCPDS card no. 36-1451, indicating a hexagonal wurtzite crystal structure [19]. The sharp and well-defined peaks further suggest the crystalline nature of the material. Distinct peaks were recorded at 2θ values of 32.9º, 34.9º, 36.8º, 48.2º, 57.3º, 63.8º, 66.8º, 68.2º, 69.3º and 73.6º, which correspond to the (100), (002), (101), (102), (110), (103), (200), (112), (201) and (202) crystallographic planes, respectively. The measured interplanar spacings

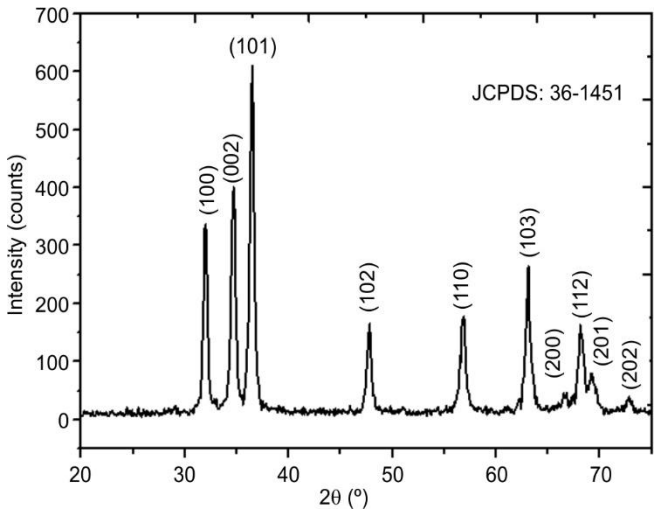


Fig. 1. XRD pattern of ZnO NPs

closely matched those calculated using Bragg's equation and were consistent with JCPDS reference data. The calculated lattice parameters for the hexagonal ZnO structure were found to be a = b = 0.3249 nm and c = 0.5206 nm. The average crystallite was calculated by Debye-Scherrer's equation:

$$D = \frac{K\lambda}{\beta \cos\theta}$$

where K = 0.9 (Scherrer's constant), λ = 0.154 nm, β = full width half maxima (FWHM) and θ = Bragg's angle. The average crystallite size was measured as 42 nm.

**Particle size distribution analysis:** The particle distribution in the solution were analyzed using a particle size analyzer based on the dynamic light scattering (DLS) theory. ZnO NPs were dispersed in ethanol with the help of an ultrasonic sonicator to examine their particle behaviour. Brownian motion effects generated histograms, from which the mean value was used to determine the average particle size of the nanoparticles. Fig. 2 illustrates the particle distribution observed in the particle size analysis, showing that the average size of the ZnO NPs is approximately 54 nm. Remarkably, the mean crystallite size is consistently smaller than overall average particle size.

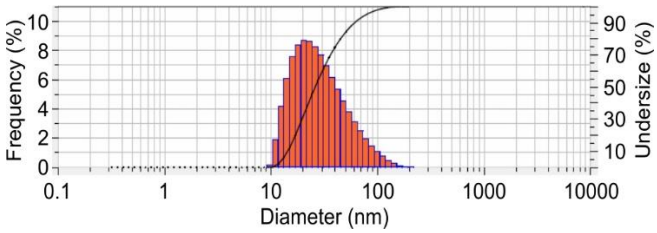


Fig. 2. Histogram of ZnO NPs

**SEM analysis:** The grain size, shape and surface morphology of the ZnO NPs were examined using a scanning electron microscope (SEM) at 1 µm and 200 nm magnification. Fig. 3a-b displays SEM images confirming the successful formation of ZnO NPs. The particles exhibit a porous morphology with an average size of approximately 200 nm. This porous structure is advantageous for applications such as seed germination, where increased surface area enhances interaction and efficiency [20].

**Energy dispersive X-ray spectroscopy (EDS):** The elemental composition of the synthesized ZnO NPs was analyzed using EDS, as illustrated in Fig. 4. The spectrum confirms the exclusive presence of zinc and oxygen in the sample, indicating high purity and the absence of detectable impurities. The corresponding quantitative data show that the nanoparticles consist of 72.22 wt.% zinc and 27.78 wt.% oxygen. These values align with the expected stoichiometry of ZnO, validating the successful synthesis of pure ZnO NPs.

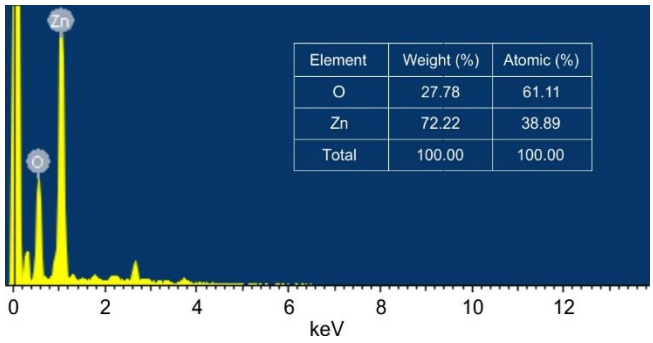


Fig. 4. EDS of ZnO NPs

**Thermal studies:** TGA and DTA were used to evaluate the ZnO NPs thermal stability. During thermal analysis, the ZnO NPs were gradually heated from room temperature to 800 ºC to analyze the weight loss and thermal events. Alumina was used as the reference material in the differential thermal analysis (DTA) to ensure accurate thermal comparison. As shown in Fig. 5, the DTA curve reveals no significant phase transitions throughout the temperature range, indicating the thermal stability of the ZnO NPs. This stability is advantageous for applications that demand high-temperature resilience [21]. Generally, weight loss is observed from room tempera-

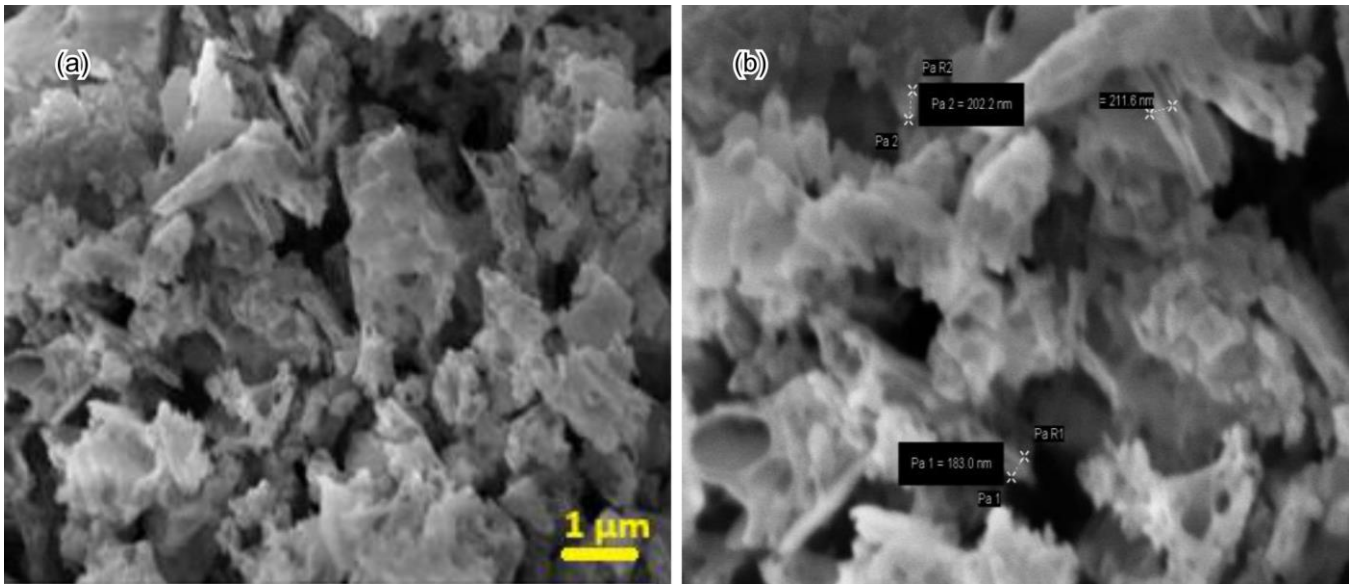


Fig. 3. SEM images of ZnO NPs (a) at 1 µm (b). 200 nm

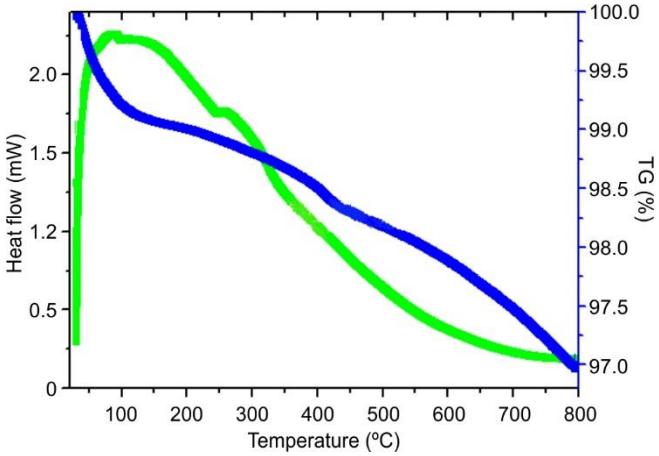


Fig. 5. TG-DTA curves of ZnO NPs

ture to 120 ºC due to the evaporation of water molecules. The weight loss obtained from 120 ºC to around 400 ºC due to the evaporation of unreacted inorganic materials in the sample. From 400 ºC to 800 ºC, the weight loss was caused by the unreacted organic solvents in the sample. The total weight loss of the nanoparticles showed 3%.

**FTIR studies:** Fig. 6 displays the FTIR spectrum of the synthesized ZnO NPs. Although FTIR is not a primary technique for characterizing purely inorganic materials, it is useful for detecting surface-bound groups or byproducts from synthesis. A distinguished absorption band around 912 $cm^{-1}$ is attributed to Zn-O stretching, supporting the presence of zinc oxide. The band observed near 1394 $cm^{-1}$ may correspond to C-O vibrations, likely originating from atmospheric carbonates or organic residues introduced during the preparation process. Moreover, the peak at 1622 $cm^{-1}$ is commonly linked to the bending vibration of adsorbed water molecules. A broad absorption around 3440 $cm^{-1}$ indicates O-H stretching, suggesting surface hydroxyl groups or moisture retention. These features confirm the formation of ZnO NPs with minor surface interactions involving moisture and trace organic compounds.

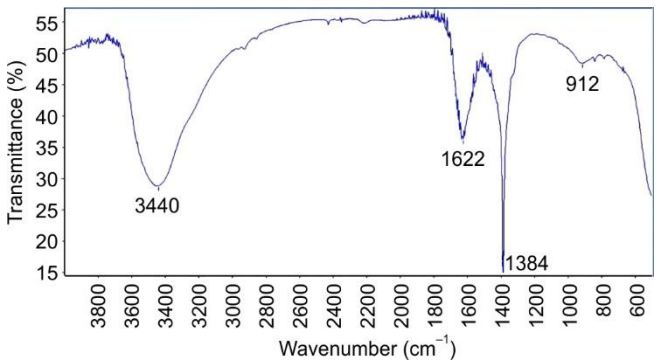


Fig. 6. FTIR spectrum of ZnO NPs

**Mung bean growth:** Seed growth was monitored and recorded daily to observe any variances in germination and development based on ZnO NPs exposure levels as shown in Fig. 7a-e. This setup provides insights into the potential influence of ZnO NPs on mung bean growth.


Fig. 7. Observation of growth of plants

The height of the plants was measured daily using a standard meter scale. Initial observations from Day 1 to Day 5 indicated growth measurements of 8 cm, 9.5 cm, 10.5 cm and 11.5 cm for Pot-1, Pot-2, Pot-3 and Pot-4, respectively as shown in Fig. 8. By Day 10, these values had increased to 14 cm, 15.5 cm, 16.5 cm and 17.5 cm across the respective pots. On Day 15, plant heights were 20 cm, 21.5 cm, 22.5 cm and 23.5 cm, while Day 20 saw final heights of 26 cm, 27.5 cm, 28.5 cm and 29.5 cm for Pot-1, Pot-2, Pot-3 and Pot-4, respectively.

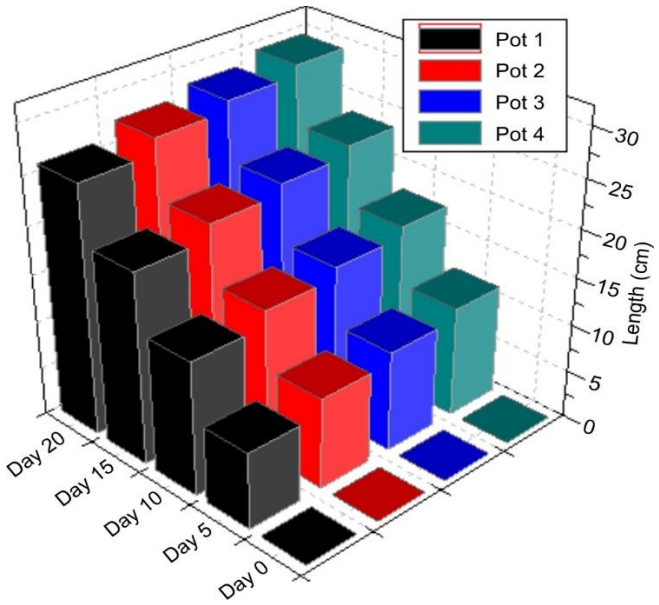


Fig. 8. Growth of plants in the function of days

From Day 10 to Day 20, growth appeared to stabilize, likely due to consistent environmental conditions. By the end of the observation period, Pot-4 demonstrated the highest growth, indicating that the plants exposed to the highest concentration of ZnO NPs (0.03 g) showed maximum development among all tested groups. By exposing *V. radiata* seeds to ZnO NPs suspensions in controlled environments, we observed distinct phytotoxic responses at different concentrations. These findings may offer valuable insights into the potential risks and benefits of ZnO NPs application in agricultural settings, particularly as their use grows in the field of agronomy and plant science [22,23].

**Effect of pH of soil in *V. radiata* cultivation treated with ZnO NPs:** The pH of soil was analyzed to assess the impact of ZnO NPs treatments on the growing conditions of *V. radiata* as shown in Fig. 9. Soil samples were collected after plant growth under varying ZnO NPs concentrations (control, 0.01 g, 0.02 g and 0.03 g) and pH values were measured. The slight increase in pH values with higher ZnO NPs concentrations may be attributed to the basic nature of ZnO NPs and their ability to interact with water, forming hydroxyl ions [24,25]. Changes in pH might influence nutrient availability, affecting seed germination and growth [26]. These findings underscore the impact of ZnO NPs on soil chemistry, emphasizing the need for careful concentration control in agricultural applications to prevent negative effects on crop productivity and soil health.

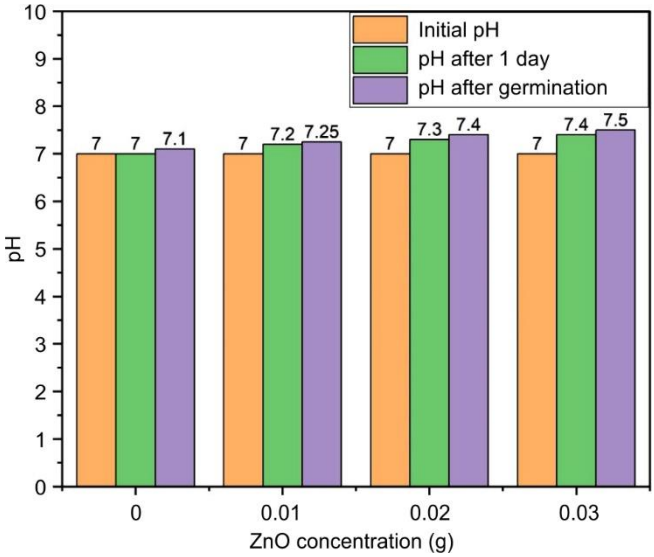


Fig. 9. pH analysis of soil in *Vigna radiata* cultivation treated with varying concentrations of ZnO NPs

**Moisture content analysis of *V. radiata* under ZnO NPs treatment:** The moisture content (MC) of *V. radiata* subjected to varying concentrations of ZnO NPs was analyzed to determine the impact of nanoparticles on water retention properties. Fresh and dry weights of plant samples from control and treated groups were measured and moisture content was calculated using the standard formula:

$$\text{Moisture content } (\%) = \frac{\text{Fresh weight} - \text{Dry weight}}{\text{Fresh weight}} \times 100$$

Fig. 10 shows a decline in moisture content with increasing concentrations of ZnO NPs, indicating that higher nanoparticles levels impair the plant's ability to retain water. This effect is likely due to nanoparticle-induced stress disrupting key physiological processes [27-29]. The observed reduction in moisture suggests alterations in cellular water balance and nutrient transport, underscoring a significant phytotoxic impact of ZnO NPs.

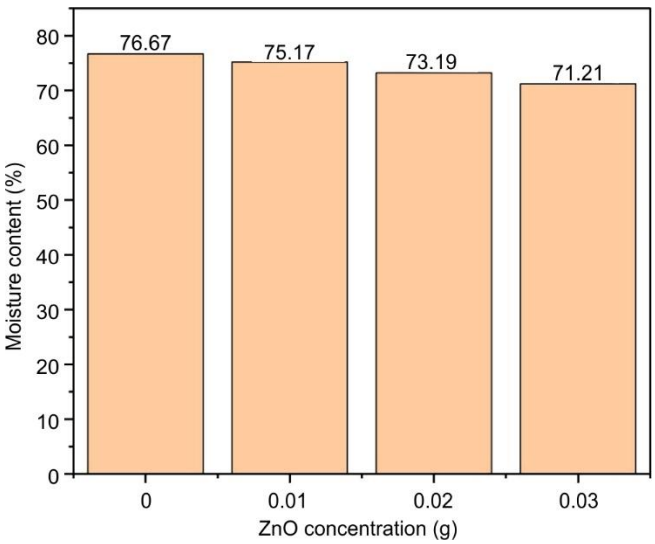


Fig. 10. Moisture content analysis of *Vigna radiata* under varying concentrations of ZnO NPs

## Conclusion

In this work, ZnO NPs were synthesized successfully using the solution combustion method. The X-ray diffraction (XRD) confirmed a hexagonal phase with a crystallite size of 42 nm, while particle size analysis indicated an average size of 54 nm. Scanning electron microscopy (SEM) revealed a porous morphology and energy-dispersive X-ray spectroscopy (EDS) verified the purity of synthesized ZnO nanoparticles. Thermogravimetric and differential thermal analysis (TG-DTA) showed a 3% weight loss with characteristic exothermic peaks, confirming the thermal stability. Germination studies using *Vigna radiata* (mung bean) seeds indicated that lower concentrations of ZnO NPs enhanced plant growth, likely due to improved nutrient availability mediated by pH changes. However, higher concentrations impaired water retention and disrupted physiological functions, suggesting the phytotoxic effects. Overall, the results highlight the potential of ZnO NPs to enhance plant growth at optimal concentrations, with important implications for sustainable agricultural applications.

## CONFLICT OF INTEREST

The authors declare that there is no conflict of interests regarding the publication of this article.

## REFERENCES


1. K.A. Altammar, *Front. Microbiol.*, **14**, 1155622 (2023); https://doi.org/10.3389/fmicb.2023.1155622
2. V. Harish, M.M. Ansari, D. Tewari, A.B. Yadav, N. Sharma, S. Bawarig, M.-L. García-Betancourt, A. Karatutlu, M. Bechelany and A. Barhoum, *J. Taiwan Inst. Chem. Eng.*, **149**, 105010 (2023); https://doi.org/10.1016/j.jtice.2023.105010
3. E.L. Irede, R.F. Awoyemi, B. Owolabi, O.R. Aworinde, R.O. Kajola, A. Hazeez, A.A. Raji, L.O. Ganiyu, C.O. Onukwuli, A.P. Onivefu and I.H. Ifijen, *RSC Adv.*, **14**, 20992 (2024); https://doi.org/10.1039/D4RA02452D
4. H. Gulab, N. Fatima, U. Tariq, O. Gohar, M. Irshad, M.Z. Khan, M. Saleem, A. Ghaffar, M. Hussain, A.K. Jan, M. Humayun, M. Motola and M.B. Hanif, *Nano-Struct. Nano-Objects*, **39**, 101271 (2024); https://doi.org/10.1016/j.nanoso.2024.101271
5. X.-Q. Zhou, Z. Hayat, D.-D. Zhang, M.-Y. Li, S. Hu, Q. Wu, Y.-F. Cao and Y. Yuan, *Processes*, **11**, 1193 (2023); https://doi.org/10.3390/pr11041193
6. M.T. Aminzai, M. Yildirim and E. Yabalak, *Talanta*, **280**, 126790 (2024); https://doi.org/10.1016/j.talanta.2024.126790
7. L. Naik Ramavathu, T.B. Narsaiah, P. Justin, S. Khasim, A.N. Kumar, N. Raghavendra, R. Ramesh and C.R. Ravikumar, *Mater. Res. Express*, **10**, 125009 (2023); https://doi.org/10.1088/2053-1591/ad184c
8. Z. Wang, S. Wang, T. Ma, Y. Liang, Z. Huo and F. Yang, *Agronomy*, **13**, 3060 (2023); https://doi.org/10.3390/agronomy13123060
9. R. Ahmed, M.K. Uddin, M.A. Quddus, M.Y.A. Samad, M.A.M. Hossain and A.N.A. Haque, *Horticulturae*, **9**, 162 (2023); https://doi.org/10.3390/horticulturae9020162
10. B.H. Kiani, I. Arshad, S. Nazir, I.A. Saleh, S.H. Kiani, N. Zomot, W.H. Al-Qahtani, A.A. Alfuraydi and M.A. Abdel-Maksoud, *J. Soil Sci. Plant Nutr.*, **24**, 5829 (2024); https://doi.org/10.1007/s42729-024-01944-1
11. M. Sorahinobar, T. Deldari, Z. Nazem Bokaeei and A. Mehdinia, *Biologia*, **78**, 951 (2022); https://doi.org/10.1007/s11756-022-01269-3
12. M. Kang, Y. Liu, Y. Weng, H. Wang and X. Bai, *Environ. Sci. Nano*, **11**, 14 (2024); https://doi.org/10.1039/D3EN00630A
13. M. Ramzan, G. Naz, A.A. Shah, M. Parveen, M. Jamil, S. Gill and H.M.A. Sharif, *Plant Physiol. Biochem.*, **196**, 130 (2023); https://doi.org/10.1016/j.plaphy.2023.01.015
14. A. Emamverdian, A. Ghorbani, Y. Li, N. Pehlivan, J. Barker, Y. Ding, G. Liu and M. Zargar, *Agronomy*, **13**, 1748 (2023); https://doi.org/10.3390/agronomy13071748
15. D.V. Francis, A.K. Abdalla, W. Mahakham, A.K. Sarmah and Z.F.R. Ahmed, *Environ. Int.*, **190**, 108859 (2024); https://doi.org/10.1016/j.envint.2024.108859
16. B. Solanki, S. Saleem and M.S. Khan, *Plant Physiol. Biochem.*, **211**, 108678 (2024); https://doi.org/10.1016/j.plaphy.2024.108678
17. S. Saleem and M.S. Khan, *Plant Physiol. Biochem.*, **194**, 146 (2023); https://doi.org/10.1016/j.plaphy.2022.11.013
18. J. Kaur and S. Rani, *AIP Conf. Proc.*, **2728**, 040011 (2023); https://doi.org/10.1063/5.0143233
19. S.S. Ashok Kumar, S. Bashir, M. Pershaanaa, F. Kamarulazam, N.M. Saidi, Z.L. Goh, I.A.W. Ma, V. Kunjunee, A. Jamaluddin, K. Ramesh, S. Ramesh, S. Ramesh and R. Manikam, *J. Mater. Sci.*, **58**, 6516 (2023); https://doi.org/10.1007/s10853-023-08413-7
20. K. Jayalakshmi, Ismayil, S. Hegde, V. Ravindrachary, G. Sanjeev, N. Mazumdar, K.M. Sindhoora, S.P. Masti and M.S. Murari, *J. Phys. Chem. Solids*, **173**, 111119 (2023); https://doi.org/10.1016/j.jpcs.2022.111119
21. N.M. Ahmad and N. Aishah Hasan, *J. Nanotechnol.*, **2023**, 9572025 (2023); https://doi.org/10.1155/2023/9572025
22. M. Kathiravan, C. Vanitha, R. Umarani, S. Marimuthu, P. Ayyadurai, K. Sathiya, M. Yuvaraj and C. Jaiby, *Agric. Res.*, (2024); https://doi.org/10.1007/s40003-024-00792-w
23. V.L. Reddy Pullagurala, I.O. Adisa, S. Rawat, B. Kim, A.C. Barrios, I.A. Medina-Velo, J.A. Hernandez-Viezcas, J.R. Peralta-Videa and J.L. Gardea-Torresdey, *Environ. Pollut.*, **241**, 1175 (2018); https://doi.org/10.1016/j.envpol.2018.06.036
24. A.I. Daniel, M. Keyster and A. Klein, *Sci. Total Environ.*, **897**, 165483 (2023); https://doi.org/10.1016/j.scitotenv.2023.165483
25. E.I. Strekalovskaya, A.I. Perfileva and K.V. Krutovsky, *Agronomy*, **14**, 1588 (2024); https://doi.org/10.3390/agronomy14071588
26. S. Ullah, M. Shaban, A.B. Siddique, A. Zulfiqar, N.S. Lali, M. Naeem-ul-Hassan, M.I. Irfan, M. Sher, M. Fayyaz ur Rehman, A. Hanbashi, F.Y. Sabei, H.M.A. Amin and A. Abbas, *J. Environ. Chem. Eng.*, **12**, 113350 (2024); https://doi.org/10.1016/j.jece.2024.113350
27. M.S. Sheteiwy, H. Shaghaleh, Y.A. Hamoud, P. Holford, H. Shao, W. Qi, M.Z. Hashmi and T. Wu, *Environ. Sci. Pollut. Res. Int.*, **28**, 36942 (2021); https://doi.org/10.1007/s11356-021-14542-w
28. J.M. Al-Khayri, R. Rashmi, R. Surya Ulhas, W.N. Sudheer, A. Banadka, P. Nagella, M.I. Aldaej, A.A.-S. Rezk, W.F. Shehata and M.I. Almaghasla, *Plants*, **12**, 292 (2023); https://doi.org/10.3390/plants12020292
29. A.R. Khan, W. Azhar, X. Fan, Z. Ulhassan, A. Salam, M. Ashraf, Y. Liu and Y. Gan, *Environ. Sci. Pollut. Res. Int.*, **30**, 110047 (2023); https://doi.org/10.1007/s11356-023-29993-6